ORIGINAL RESEARCH

Analytical bifurcation behaviors of a host–parasitoid model with Holling type III functional response

Ahmed M. Yousef, Saad Z. Rida and Soheir Arafat*

*Correspondence:
soheiraboelnaga@gmail.com

Mathematics Department,
Faculty of Science, South Valley
University, Qena, Egypt

Abstract

This topic presents a study on a host–parasitoid model with a Holling type III functional response. In population dynamics, when host density rises, the parasitoid response initially accelerates due to the parasitoid's improved searching efficiency. However, above a certain density threshold, the parasitoid response will reach a saturation level due to the influence of reducing the handling time. Thus, we incorporated a Holling type III functional response into the model to characterize such a phenomenon. The dynamics of the current model are discussed in this paper. We first obtained the existence and local stability conditions of the positive fixed point of the model. Furthermore, we investigated the bifurcation behaviors at the positive fixed point. More specifically, we used bifurcation theory and the center manifold theorem to prove that the model possess both period doubling and Neimark–Sacker bifurcations. Then, the chaotic behavior of the model, in the sense of Marotto, is proven. Furthermore, we apply a state-delayed feedback control strategy to control the complex dynamics of the present model. Finally, numerical examples are provided to support our analytic results.

Keywords: Host–parasitoid model, Holling type III functional response, Stability, Bifurcation analysis, Chaotic behavior

Introduction

In recent decades, discrete-time models have been an interesting topic for researchers due to their ability to exhibit a wide range of complicated dynamic behavior, including various forms of bifurcations, periodic orbits, and chaotic attractors [1–4]. These discrete-time models provide an idealistic description of the dynamics of species that breed seasonally [5–8]. Also, in mathematical biology, discrete-time models are better than continuous-time models for populations with generations that do not overlap in their progeny. Furthermore, recurrence equations can be numerically investigated using rapidly evolving computer software.

The dynamic interaction between hosts and their parasitoids has been and will remain a dominant ecological subject because of its universal existence. The first difference equation model of host–parasitoid interaction was formulated by Thompson [9] in 1924s. Thompson's model has some deficiencies, such as persistence and the

existence of a positive steady-state. So, the Nicholson-Bailey model [6] was suggested to avoid these deficiencies. Nicholson-Bailey model is described as follows

$$\begin{cases} H_{n+1} = eH_n\exp(-aP_n), \\ P_{n+1} = \alpha H_n[1 - \exp(-aP_n)], \end{cases} \tag{1}$$

where H_n and P_n indicate the host and parasitoid densities respectively at generation n. The probability that a host will escape parasitism is defined by the function $\exp(-aP_n)$ generated by the Poisson distribution as suggested by Nicholson and Bailey [6], where a is the parasitoid searching efficiency, e is the mean number of eggs laid by a host, and α is the parasite's average number of progeny from a parasitized host.

A series of studies determining the subsequent evolution of model (1) were noted. For example, Yousef et al. [10] investigated the influence of mutual interference on a host–parasitoid model with Beverton–Holt growth. Their results suggested that mutual interference could be an important stabilizing factor. Liu et al. [11] established a discrete host–parasitoid model with Allee effect and Holling type III functional response. They concluded that the Allee effect can decrease the dynamic complexity of the model. Wu and Zhao [12] discussed the qualitative behaviors of a discrete host–parasitoid model with refuge and strong Allee effects. They observed that the incorporation of both refuges and strong Allee effects has either a negative or positive impact on the coexistence of the two populations. Din et al. [13] studied the qualitative behavior of a modified host–parasitoid model. Din et al. [14] constructed a new density-dependent host–parasitoid model by introducing the Hassell growth function in the host population. Yu et al. [15] studied numerically the complex dynamical behavior in a parasitoid- host–parasitoid model. Their results demonstrated that the superiority coefficient may be a strong destabilizing factor. Ringel et al. [16] investigated the evolution of a diapause in a coupled host–parasitoid system using a discrete-generation population dynamic model that incorporates the diapause. Zhao et al.[17]. investigated the effect of prolonged diapause on host–parasitoid dynamics. They concluded that the prolonged diapause may have a minor effect on the stability and persistence of coupled host–parasitoid interactions. Liu et al. [18] proposed a new host-parasitoid model with Allee effect for the host and parasitoid aggregation. Their results suggested that Allee effect can alleviate dynamic complexities. In [19], Zhao et al. suggested and numerically investigated a host–parasitoid model with prolonged diapause for the host. The researchers discovered that parasitism and moderate prolonged diapause can help the model coexist.

It is well known that functional response function between species is an important point in population dynamics research. The functional response describes the per capita parasitism rates of the parasites depending on the host density. There are four forms of functional responses, called Holling types (I, II, III, and IV), which were suggested by Holling [20]. In this work, we will study the dynamics of the host–parasitoid model by using Holling type III functional response. Holling type III functional response defines that when the host population increases, the response first rises due to the parasitoid's improved efficiency. It then decreases under the effect of handling time or satiation [21].

In this paper, we consider the following host–parasitoid model with a simplified Holling type III functional response [20, 21]:

$$\begin{cases} H_{n+1} = H_n \exp\left[r\left(1 - \frac{H_n}{K}\right) - \frac{bTH_n^2 P_n}{1 + bT_h H_n^2}\right], \\ P_{t+1} = \alpha H_n \left[1 - \exp\left(-\frac{bTH_n^2 P_n}{1 + bT_h H_n^2}\right)\right], \end{cases} \qquad (2)$$

where K is the carrying capacity for the host in the absence of parasitoid, r is the intrinsic growth rate, b is a conversion factor related to the Holling type III functional response, T is the total time initially available for search, and T_h is the handing time. The parameters b, r, K, T, T_h are all positive constants. For simplicity, we substitute $x = \frac{H}{K}$, $y = P$, $m = \frac{T}{KT_h}$, $d = \frac{1}{KbT_h}$ and $\hat{\alpha} = \alpha K$ and ignoring the hat, then model (2) can be rewritten as:

$$\begin{cases} x_{n+1} = x_n \exp\left[r(1 - x_n) - \frac{mx_n^2 y_n}{d + x_n^2}\right], \\ y_{n+1} = \alpha x_n \left[1 - \exp\left(-\frac{mx_n^2 y_n}{d + x_n^2}\right)\right], \end{cases} \qquad (3)$$

where x_n and y_n indicate the host and parasitoid densities respectively at generation n. The term $\frac{mx_n^2 y_n}{d + x_n^2}$ is Holling type III functional response. In population dynamics, the Holling Type III functional response is used to simulate the switching phenomenon [22]. The sigmoidal nature of this functional response frequently indicates an instance of learning behavior in the parasitoid population, with a monotonic increase in the success rate of parasitism as more interactions with the host take place [20]. Incorporating a Holling Type III functional response into the Neclison-Billey model has the potential to maintain a more stable host–parasitoid balance.

The purpose of this work is to highlight the analysis of dynamic complexity in a discrete-time host–parasitoid model with Hollings Type III functional response. That is, we will investigate how the Holling type III response influences the dynamic complexity of host–parasitoid interactions.

The major contribution of this research is to examine the dynamic behaviors of the host–parasitoid model with Hollings Type III functional response. As far as we know, there has not been any research that has focused on the examination of qualitative behaviors in the current model. As a result, we first used an effective technique to discuss the analytical bifurcation structures of two-dimensional discrete-time models [8]. It is entirely independent of any symmetry technique or numerical bifurcation tools. More specifically, we study flip and Neimark–Sacker bifurcation analytically for the first time using normal form theory and the center manifold theorem. In addition, sensitivity alone is insufficient for deducing the onset of chaotic behaviors in some ecological models. Thus, we exhibited the first strict evidence for Marotto's chaos existence in the host–parasitoid model with Holling Type III functional response by using the snap-back repeller concept. Also, our results suggest that the ecological model is more likely to stay stable if we choose a good functional response.

The following is the layout of the paper: in Sect. Methods, the boundedness and existence of the positive fixed point of the model are investigated. Then, the local stability of the model fixed point is discussed. Furthermore, a detailed analysis of the bifurcation of fixed points is studied. Then, we derived the conditions for the existence

Yousef *et al. Journal of the Egyptian Mathematical Society* (2023) 31:2

Page 4 of 22

of Marotto's chaos. After that, we apply a stated-delayed feedback control strategy to eliminate the bifurcation and chaotic behavior of our model. In Sect. Results and discussion, numerical simulations are performed to validate the theoretical results. A brief conclusion is presented in Sect. Conclusion.

Methods

Existence and boundedness of positive fixed point

First, we show the boundedness of the model (3) and the existence of a positive fixed point as follows:

Lemma 1 [23] *Suppose that x_n satisfies $x_0 > 0$, and $x_{n+1} \leq x_n \exp[A(1 - Bx_n)]$ for $n \in N$, where A and B are positive constants. Then $\lim_{n \to \infty} \sup x_n \leq \frac{1}{AB} \exp(A - 1)$.*

Theorem 1 *Every positive solution (x_n, y_n) of model (3), satisfies the following inequality:* $\lim_{n \to \infty} \sup(x_n, y_n) \leq \max\left\{\frac{1}{r} \exp(r - 1), \frac{\alpha}{r} \exp(r - 1)\right\}$.

Proof:

Suppose that $\{(x_n, y_n)\}$ is a positive arbitrary solution of model (3). Next, from the first equation of model (3), we get.

$$
\begin{aligned}
x_{n+1} &= x_n \exp\left[r(1 - x_n) - \frac{mx_n^2 y_n}{d + x_n^2}\right] \\
&\leq x_n \exp[r(1 - x_n)],
\end{aligned}
$$

for all $n = 0, 1, 2, \cdots$. Suppose that $x_0 > 0$, then by using Lemma 1, we acquire

$$
\lim_{n \to \infty} \sup x_n \leq \frac{1}{r} \exp(r - 1). \tag{4}
$$

In the similar manner, from the second equation of model (3), one concludes

$$
\begin{aligned}
y_{n+1} &= \alpha x_n \left[1 - \exp\left(-\frac{mx_n^2 y_n}{d + x_n^2}\right)\right] \\
&\leq \alpha \lim_{n \to \infty} \sup x_n \leq \frac{\alpha}{r} \exp(r - 1).
\end{aligned} \tag{5}
$$

Thus, it follows that $\lim_{n \to \infty} \sup(x_n, y_n) \leq \max\left\{\frac{1}{r} \exp(r - 1), \frac{\alpha}{r} \exp(r - 1)\right\}$.

Theorem 2 *If $d + 1 < m\alpha$, the model (3) has a positive fixed point $(x_*, y_*) \in (0, 1)$.*

Proof:

The fixed point can be obtained by solving.

$$
x = x \exp\left[r(1 - x) - \frac{mx^2 y}{d + x^2}\right], \quad y = \alpha x \left[1 - \exp\left(-\frac{mx^2 y}{d + x^2}\right)\right].
$$

Ignoring the trivial fixed point $(0, 0)$, *so that we are left with*

$$y = \frac{r(d + x^2)(1 - x)}{mx^2}, \quad x = \frac{y}{\alpha\left[1 - \exp\left(-\frac{mx^2 y}{d + x^2}\right)\right]}.$$

Suppose that

$$F(x) := \frac{f(x)}{\alpha[1 - \exp(r(x - 1))]} - x,$$

where $f(x) = \frac{r(d + x^2)(1 - x)}{mx^2}$. *Then,*

$$\lim_{x \to 0^+} F(x) = \lim_{x \to 0^+} \left\{ \frac{f(x)}{\alpha[1 - \exp(r(x - 1))]} - x \right\} = +\infty.$$

Notice that, $f(1) = 0$. *By applying l'Hôpital's rule, and assume that* $d + 1 < m\alpha$, *we get*

$$\lim_{x \to 1^-} F(x) = \lim_{x \to 1^-} \left\{ \frac{f'(x)}{-\alpha r \exp(r(x - 1))} - 1 \right\} = \frac{d + 1}{m\alpha} - 1 < 0,$$

So, $F(x) = 0$ *has at least one positive root in* $(0, 1)$.

Stability analysis of the positive fixed point

Now, we study the conditions of local stability of the positive fixed point $E_*(x_*, y_*)$. First, the generalized Jacobian matrix of model (3) evaluated at $E_*(x_*, y_*)$ is given by:

$$J(E_*) = \begin{pmatrix} \left(1 - rx_* - \frac{2dmx_*^2 y_*}{(d + x_*^2)^2}\right)\exp\left[r(1 - x_*) - \frac{mx_*^2 y_*}{d + x_*^2}\right] & \frac{-mx_*^3}{d + x_*^2}\exp\left[r(1 - x_*) - \frac{mx_*^2 y_*}{d + x_*^2}\right] \\ \alpha\left[1 - \exp\left(\frac{-mx_*^2 y_*}{d + x_*^2}\right)\right] + \frac{2md\alpha x_*^2 y_*}{(d + x_*^2)^2}\exp\left(-\frac{mx_*^2 y_*}{d + x_*^2}\right) & \frac{-mx_*^3}{d + x_*^2}\exp\left[r(1 - x_*) - \frac{mx_*^2 y_*}{d + x_*^2}\right] \end{pmatrix}$$

The characteristic equation of $J(x_*, y_*)$ can be written as:

$$P(\lambda) = \lambda^2 + R(x_*, y_*)\lambda + Q(x_*, y_*), \tag{6}$$

where

$$R(x_*, y_*) = -\left[1 - rx_* - \frac{2dmx_*^2 y_*}{(d + x_*^2)^2} + \frac{mx_*^2}{d + x_*^2}(\alpha x_* - y_*)\right], \tag{7}$$

and

$$Q(x_*, y_*) = \frac{\alpha mx_*^3}{d + x_*^2} - \frac{mrx_*^3}{(d + x_*^2)}(\alpha x_* - y_*). \tag{8}$$

For the discussion of the stability of the fixed point $E_*(x_*, y_*)$, we state the next lemma [24].

Lemma 2 [25] *Take the second-degree polynomial equation*

$$\lambda^2 + \hat{A}\lambda + \hat{B} = 0, \tag{9}$$

where $\hat{A}$ and $\hat{B}$ are both real values. Then,

$$\left|\hat{A}\right| < 1 + \hat{B} < 2,$$

is the necessary and sufficient condition for both roots of the (9) *to lie inside the open disk* $|\lambda| < 1$.

Proposition 1 *Let $E_*\left(x_*, y_*\right)$ be the positive fixed point of model* (3). *Then, the next statements hold*:

1. *$E_*\left(x_*, y_*\right)$ is a repeller if and only if*

   $$\left|Q\left(x_*, y_*\right)\right| > 1, \text{ and } \left|R\left(x_*, y_*\right)\right| < \left|1 + Q\left(x_*, y_*\right)\right|.$$

2. *$E_*\left(x_*, y_*\right)$ is a saddle point if and only if*

   $$R\left(x_*, y_*\right)^2 > 4Q\left(x_*, y_*\right), \quad \left|R\left(x_*, y_*\right)\right| > \left|1 + Q\left(x_*, y_*\right)\right|.$$

3. *$E_*\left(x_*, y_*\right)$ is a non-hyperbolic point if and only if*

   $$\left|R\left(x_*, y_*\right)\right| = \left|1 + Q\left(x_*, y_*\right)\right|, \tag{10}$$

Or

$$Q\left(x_*, y_*\right) = 1 \text{ and } \left|R\left(x_*, y_*\right)\right| \le 2. \tag{11}$$

The theorem below demonstrates the necessary and adequate conditions for the local asymptotic stability of the model (3) *at its positive fixed point.*

Theorem 3 *If neither* (10) *nor* (11) *holds, then the positive fixed point of* (3) *is locally asymptotically stable if and only if*

$$\left|R\left(x_*, y_*\right)\right| < 1 + Q\left(x_*, y_*\right) < 2,$$

where $R\left(x_*, y_*\right)$ and $Q\left(x_*, y_*\right)$ are given in (7) *and* (8), *respectively.*

Bifurcation analysis

Now, we will discuss different bifurcation types [26, 27] of the model (3). Recall the characteristic equation of $J(E_*)$:

$$P(\lambda) = \lambda^2 - R(x_*, y_*)\lambda + Q(x_*, y_*), \tag{12}$$

where

$$R(x_*, y_*) = 1 - rG - L + V, \quad Q(x_*, y_*) = N - rGV,$$

and

$$G = x_*, \quad L = \frac{2dmx_*^2 y_*}{(d + x_*^2)^2}, \quad V = \frac{mx_*^2}{d + x_*^2}(\alpha x_* - y_*), \quad N = \frac{\alpha m x_*^3}{d + x_*^2}.$$

If $R^2(x_*, y_*) > 4Q(x_*, y_*)$, that is:

$$(1 - rG - L + V)^2 > 4(N - rGV), \tag{13}$$

and $R(x_*, y_*) + Q(x_*, y_*) = -1$, then

$$r = \frac{2 - L + V + N}{G + GV}. \tag{14}$$

So, the eigenvalues of $E_*(x_*, y_*)$ is $\lambda_1 = -1$ and $\lambda_2 = 2 - rG - L + V$.
Consider

$$\Omega_{FB} = \left\{(r, d, m, \alpha) \in R_+^4 : (13) \, and \, (14) \, are \, satisfied \, \lambda_2 = 2 - rG - L + V \right\},$$

and

$$\Omega_{NS} = \{(r, d, m, \alpha) \in R_+^4 : r = \frac{N - 1}{GV}, \quad |1 - rG - L + V| < 2\}.$$

Flip bifurcation

Firstly, we investigate the flip bifurcation of model (3) when the parameters vary in a small neighborhood of Ω_{FB}. Taking arbitrary parameters (r_1, d, m, α) from Ω_{FB}, then model(3) is converted to

$$\begin{cases} x \rightarrow x \exp\left[r_1(1 - x) - \frac{mx^2 y}{d + x^2}\right] \\ y \rightarrow \alpha x \left[1 - \exp\left(-\frac{mx^2 y}{d + x^2}\right)\right]. \end{cases} \tag{15}$$

Choosing r_1 as a bifurcation parameter. Model (15) has a positive fixed point $E_*(x_*, y_*)$ which may undergoes a flip bifurcation when r_1 varies in a small neighborhood of Ω_{FB}.

Consider a small perturbation of (15) as follows:

$$\begin{cases} x \to x\exp\left[(r^* + r_1)(1 - x) - \frac{mx^2y}{d+x^2}\right] \\ y \quad\quad \to \alpha x\left[1 - \exp\left(-\frac{mx^2y}{d+x^2}\right)\right], \end{cases} \tag{16}$$

where $|r^*| \ll 1$, denotes a small perturbation parameter.

Assume $u = x - x_*$ and $v = y - y_*$, then model (16) becomes

$$\begin{pmatrix} u \\ v \end{pmatrix} \to \begin{pmatrix} a_1 & a_2 \\ b_1 & b_2 \end{pmatrix}\begin{pmatrix} u \\ v \end{pmatrix} + \begin{pmatrix} f_1(u,v,r^*) \\ g_1(u,v,r^*) \end{pmatrix}, \tag{17}$$

where

$$\begin{aligned} f_1(u,v,r^*) &= a_{13}ur^* + a_{11}u^2 + a_{22}v^2 + a_{113}u^2r^* + a_{1133}u^2r^{*2} \\ &\quad + a_{12}uv + a_{123}uvr^* + O\Big((|u| + |v| + |r^*|)^3\Big), \\ g_1(u,v,r^*) &= b_{11}u^2 + b_{12}uv + b_{22}v^2 + O\Big((|u| + |v| + |r^*|)^3\Big), \end{aligned}$$

$$a_1 = 1 - r_1 G - L, \quad a_2 = -\frac{N}{\alpha}, \quad a_{13} = -G, \quad a_{22} = \frac{m^2 x_*^3}{\left(d + x_*^2\right)^2},$$

$$a_{113} = r_1 x_* - 1 + \frac{2mdx_*^2 y_*}{\left(d + x_*^2\right)^2}, \quad a_{1133} = G, \quad a_{123} = \frac{mx_*^3}{K\left(d + x_*^2\right)},$$

$$a_{11} = -2r_1 + r_1^2 x_* + \frac{2(mdy)_*^2 x_*^3 - 2md^3 x_* y_* - 2mdx_*^3 y_*}{\left(d + x_*^2\right)^4} + \frac{mdr_1 x_*^2 y_* + r_1 mdx_*^2 y_* - mdx_* y_*}{\left(d + x^2\right)_*^2},$$

$$a_{12} = \frac{2mdx_*^4 y_* - 2mdx_*^2\left(d + x_*^2\right) + \left(mr^1 x_*^3 - mx_*^2\right)\left(d + x_*^2\right)^2}{\left(d + x_*^2\right)^3},$$

$$b_1 = \frac{y_*}{x_*} + \frac{2mdx_* y_*}{\left(d + x_*^2\right)^2}\left(\alpha x_* - y_*\right), \quad b_2 = V, \quad b_{22} = \frac{-V^2}{\left(\alpha x_* - y_*\right)},$$

$$b_{11} = \left[\frac{2md_*^3 y_* - 2mdx_*^4 y_* - 2(mdy_*)^2 x_*^2 + mdy_*\left(d + x_*^2\right)^2}{\left(d + x_*^2\right)^4}\right]\left(\alpha x_* - y_*\right),$$

$$b_{12} = \left[\frac{3mx_*\left(d + x_*^2\right) - 2mx_*^3}{2\left(d + x_*^2\right)^2} - \frac{dm^2 x_*^3 y_*}{2\left(d + x_*^2\right)^3}\right]\left(\alpha x_* - y_*\right). \tag{18}$$

We next consider the following nonsingular matrix

$$T = \begin{pmatrix} a_2 & a_2 \\ -1 - a_1 & \lambda_2 - a_1 \end{pmatrix}.$$

Using the following translation

$$\begin{pmatrix} u \\ v \end{pmatrix} = T\begin{pmatrix} \tilde{x} \\ \tilde{y} \end{pmatrix}, \tag{19}$$

Then, the model (17) becomes

$$\begin{pmatrix} \tilde{x} \\ \tilde{y} \end{pmatrix} \to \begin{pmatrix} -1 & 0 \\ 0 & \lambda_2 \end{pmatrix}\begin{pmatrix} \tilde{x} \\ \tilde{y} \end{pmatrix} + \begin{pmatrix} f_2(\tilde{x}, \tilde{y}, r^*) \\ g_2(\tilde{x}, \tilde{y}, r^*) \end{pmatrix}, \tag{20}$$

where

$$
\begin{aligned}
f_2\left(\tilde{x}, \tilde{y}, r^*\right) = & \frac{a_{13}(\lambda_2 - a_1)}{a_2(1 + \lambda_2)} u r^* + \left(\frac{a_{11}(\lambda_2 - a_1)}{a_2(1 + \lambda_2)} - \frac{b_{11}}{1 + \lambda_2}\right) u^2 \\
& + \left(\frac{a_{22}(\lambda_2 - a_1)}{a_2(1 + \lambda_2)} - \frac{b_{22}}{1 + \lambda_2}\right) v^2 + \frac{a_{113}(\lambda_2 - a_1)}{a_2(1 + \lambda_2)} u^2 r^* \\
& + \frac{a_{1113}(\lambda_2 - a_1)}{a_2(1 + \lambda_2)} u^2 r^{*2} + \left(\frac{a_{12}(\lambda_2 - a_1)}{a_2(1 + \lambda_2)} - \frac{b_{12}}{1 + \lambda_2}\right) uv \\
& + \frac{a_{123}(\lambda_2 - a_1)}{a_2(1 + \lambda_2)} uv r^* + O\left(\left(|u| + |v| + |r^*|\right)^3\right), \\
g_2\left(\tilde{x}, \tilde{y}, r^*\right) = & \frac{a_{13}(1 + a_1)}{a_2(1 + \lambda_2)} u r^* + \left(\frac{a_{11}(1 + a_1)}{a_2(1 + \lambda_2)} + \frac{b_{11}}{1 + \lambda_2}\right) u^2 \\
& + \left(\frac{a_{22}(1 + a_1)}{a_2(1 + \lambda_2)} + \frac{b_{22}}{1 + \lambda_2}\right) v^2 + \frac{a_{113}(1 + a_1)}{a_2(1 + \lambda_2)} u^2 r^* \\
& + \frac{a_{1113}(1 + a_1)}{a_2(1 + \lambda_2)} u^2 r^{*2} + \left(\frac{a_{12}(1 + a_1)}{a_2(1 + \lambda_2)} + \frac{b_{12}}{1 + \lambda_2}\right) uv \\
& + \frac{a_{123}(1 + a_1)}{a_2(1 + \lambda_2)} uv r^* + O\left(\left(|u| + |v| + |r^*|\right)^3\right),
\end{aligned}
$$

and

$$
\begin{aligned}
& u = a_2(\tilde{x} + \tilde{y}), \quad v = (-1 - a_1)\tilde{x} + (\lambda_2 - a_1)\tilde{y}, \\
& u^2 = a_2^2\left(\tilde{x}^2 + 2\tilde{x}\tilde{y} + \tilde{y}^2\right), \\
& uv = a_2\left[-(1 + a_1)\tilde{x}^2 + (\lambda_2 - 1 - 2a_1)\tilde{x}\tilde{y} + (\lambda_2 - a_1)\tilde{y}^2\right], \\
& v^2 = (1 + a_1)^2\tilde{x}^2 - 2(1 + a_1)(\lambda_2 - a_1)\tilde{x}\tilde{y} + (\lambda_2 - a_1)^2\tilde{y}^2.
\end{aligned}
$$

Assume that Eq. (20) has a center manifold $W^c(0, 0, 0)$ at $r^* = 0$, which may be approximated as below [11]:

$$
W^c(0, 0, 0) = \left\{(\tilde{x}, \tilde{y}, r^*) \in R^3; \tilde{y} = l_1\tilde{x}^2 + l_2\tilde{x}a^* + l_3 r^{*2} + O\left(\left(|\tilde{x}| + |r^*|\right)^3\right)\right\},
$$

where

$$
\begin{aligned}
l_1 & = \frac{a_2 a_{11}(1 + a_1) + b_{11}a_2^2}{1 - \lambda_2^2} - \frac{a_{12}(1 + a_1)^2 + a_2 b_2(1 + a_1)}{1 - \lambda_2^2} + \frac{a_{22}(1 + a_1)^3 + a_2 b_{22}(1 + a_1)^2}{a_2\left(1 - \lambda_2^2\right)}, \\
l_2 & = \frac{-a_{13}(1 + a_1)}{(1 + \lambda_2)^2}, \\
l_3 & = 0.
\end{aligned}
$$

Therefore, the model (20) restricted to the center manifold $W^c(0, 0, 0)$ given by

$$
F : \tilde{x} \rightarrow -\tilde{x} + s_1\tilde{x}^2 + s_2\tilde{x}r^* + s_3\tilde{x}^2 r^* + s_4\tilde{x}r^{*2} + s_5\tilde{x}^3 + O\left(\left(|\tilde{x}| + |r^*|\right)^4\right),
$$

where

$$s_1 = a_2^2 \left[\frac{a_{11}(\lambda_2 - a_1)}{a_2(1 + \lambda_2)} - \frac{b_{11}}{1 + \lambda_2} \right] - a_2(1 + a_1) \left[\frac{a_{12}(\lambda_2 - a_1)}{a_2(1 + \lambda_2)} - \frac{b_{12}}{1 + \lambda_2} \right]$$
$$+ (1 + a_1)^2 \left[\frac{a_{22}(\lambda_2 - a_1)}{a_2(1 + \lambda_2)} - \frac{b_{22}}{1 + \lambda_2} \right],$$

$$s_2 = a_2(1 + l_2) \left[\frac{a_{13}(\lambda_2 - a_1)}{a_2(1 + \lambda_2)} \right],$$

$$s_3 = 2a_2^2 l_2 \left(\frac{a_{11}(\lambda_2 - a_1)}{a_2(1 + \lambda_2)} - \frac{b_{11}}{1 + \lambda_2} \right) + a_2 l_2(\lambda_2 - 2a_1 - 1) \left[\frac{a_{12}(\lambda_2 - a_1)}{a_2(1 + \lambda_2)} - \frac{b_{12}}{1 + \lambda_2} \right]$$
$$- 2l_2(1 + a_1)(\lambda_2 - a_1) \left[\frac{a_{22}(\lambda_2 - a_1)}{a_2(1 + \lambda_2)} - \frac{b_{22}}{1 + \lambda_2} \right] + a_2 l_1 \left(\frac{a_{13}(\lambda_2 - a_1)}{a_2(1 + \lambda_2)} \right)$$
$$- a_2(1 + a_1) \left[\frac{a_{123}(\lambda_2 - a_1)}{a_2(1 + \lambda_2)} \right] + a_2^2 \left[\frac{a_{113}(\lambda_2 - a_1)}{a_2(1 + \lambda_2)} \right],$$

$$s_4 = a_2 l_2 \left[\frac{a_{13}(\lambda_2 - a_1)}{a_2(1 + \lambda_2)} \right],$$

$$s_5 = 2a_2^2 l_1 \left(\frac{a_{11}(\lambda_2 - a_1)}{a_2(1 + \lambda_2)} \right) + a_2 l_1(\lambda_2 - 2a_1 - 1) \left[\frac{a_{12}(\lambda_2 - a_1)}{a_2(1 + \lambda_2)} - \frac{b_{12}}{1 + \lambda_2} \right]$$
$$- 2l_1(1 + a_1)(\lambda_2 - a_1) \left[\frac{a_{22}(\lambda_2 - a_1)}{a_2(1 + \lambda_2)} - \frac{b_{22}}{1 + \lambda_2} \right].$$

Define the following two nonzero real quantities:

$$\alpha_1 = \left(2 \frac{\partial^2 F}{\partial \tilde{x} \partial r^*} + \frac{\partial F}{\partial r^*} \frac{\partial F}{\partial \tilde{x}} \right)_{(0,0)} = 2s_2 \neq 0,$$

$$\alpha_2 = \left(\frac{1}{2} \left(\frac{\partial^2 F}{\partial \tilde{x}^2} \right)^2 + \frac{1}{3} \left(\frac{\partial^3 F}{\partial \tilde{x}^3} \right) \right)_{(0,0)} = 2 \left(s_1^2 + s_3 \right) \neq 0.$$

Finally, the above discussion can be summarized in the next theorem.

Theorem 4   *When the parameter r fluctuates in a small neighborhood of r_1, the model (3) undergoes a flip bifurcation at the fixed point (x_*, y_*) if $\alpha_2 \neq 0$. Moreover, if $\alpha_2 > 0$, the period-2 orbits bifurcating from (x_*, y_*) are stable, whereas if $\alpha_2 < 0$, they are unstable.*

Neimark–Sacker bifurcation

Secondly, we discuss the Neimark–Sacker bifurcation of model (3) by choosing the parameters (d, r_2, m, α) arbitrarily from the set Ω_{NS}, so, model (3) is converted into the new following form:

$$\begin{pmatrix} x \\ y \end{pmatrix} \rightarrow \begin{pmatrix} x \exp\left[r_2(1 - x) - \frac{mx^2 y}{d + x^2} \right] \\ \alpha x \left[1 - \exp\left(-\frac{mx^2 y}{d + x^2} \right) \right] \end{pmatrix}. \tag{21}$$

Consider a perturbation of (21) as below:

$$\begin{pmatrix} x \\ y \end{pmatrix} \rightarrow \begin{pmatrix} x\exp\left[(\overline{r^*} + r_2)(1 - x) - \frac{mx^2 y}{d + x^2}\right] \\ \alpha x\left[1 - \exp\left(-\frac{mx^2 y}{d + x^2}\right)\right] \end{pmatrix} \tag{22}$$

where $\left|\overline{r^*}\right| \ll 1$ denotes a small perturbation parameter.

Suppose $u = x - x_*$, $v = y - y_*$. Then, we transform the fixed point (x_*, y_*) of model (22) into the origin, we have

$$\begin{pmatrix} u \\ v \end{pmatrix} \rightarrow \begin{pmatrix} a_1 u + a_2 v + a_{11} u^2 + a_{12} uv + a_{22} v^2 + O\left((|u| + |v|)^3\right) \\ b_1 u + b_2 v + b_{11} u^2 + b_{12} uv + b_{22} v^2 + O\left((|u| + |v|)^3\right) \end{pmatrix}, \tag{23}$$

and $a_1, a_2, a_{11}, a_{12}, a_{22}, b_1, b_2, b_{11}, b_{22}, b_{12}$ are given in (19) by replacing r_1 with $r_2 + \overline{r^*}$
.

The characteristic equation of model (23) is indicated by

$$\lambda^2 - R(\overline{r^*})\lambda + Q(\overline{r^*}) = 0,$$

where

$$R(\overline{r^*}) = 1 - (r_2 + \overline{r^*})G - L + V, \quad Q(\overline{r^*}) = N - (r_2 + \overline{r^*})GV.$$

Since the parameters $(r_2, m, d, \alpha) \in NS$, then the eigenvalues are conjugate complex numbers λ, $\overline{\lambda}$ with $|\lambda, \overline{\lambda}| = 1$, where:

$$\lambda, \overline{\lambda} = \frac{R(\overline{r^*})}{2} \pm \frac{i}{2}\sqrt{4Q(\overline{r^*}) - R^2(\overline{r^*})},$$

So, we have

$$|\lambda|_{\overline{r^*}=0} = \sqrt{Q(0)} = 1, \quad l = \frac{d|\lambda|}{d\overline{r^*}}\bigg|_{\overline{r^*}=0} = \frac{-GV}{2} < 0.$$

Since the parameter $(d, r_2, m, \alpha) \in NS$, implies that $R(0) \neq -2, 2$. Thus $R(0) \neq -2, 0, 1, 2$ at $\overline{r^*} = 0$, gives $\lambda^n, \overline{\lambda}^n \neq 1$, for all $n = 1, 2, 3, 4$. Moreover, we rule out $R(0) \neq 0, 1$, which results in:

$$1 - r_2 G - L + V \neq 0, 1. \tag{24}$$

Consequently, when $\overline{r^*} = 0$ and the conditions (24) holds, the roots of (23) do not lie in the intersection of the unit circle with the coordinate axes. we use

$$\overline{r^*} = 0, \quad \mu = \frac{R(0)}{2}, \quad \omega = \frac{1}{2}\sqrt{4Q(0) - R^2(0)},$$

to generate the normal form of model (23) at $\overline{r^*} = 0$.

Consider the next translation:

$$\begin{pmatrix} u \\ v \end{pmatrix} = \begin{pmatrix} a_2 & 0 \\ \mu - a_1 & -\omega \end{pmatrix}\begin{pmatrix} \tilde{x} \\ \tilde{y} \end{pmatrix}. \tag{25}$$

Under the translation (25), we get

$$\begin{pmatrix} \tilde{x} \\ \tilde{y} \end{pmatrix} \rightarrow \begin{pmatrix} \mu & -\omega \\ \omega & \mu \end{pmatrix} \begin{pmatrix} \tilde{x} \\ \tilde{y} \end{pmatrix} + \begin{pmatrix} \overline{f_2}(\tilde{x}, \tilde{y}) \\ \overline{g_2}(\tilde{x}, \tilde{y}) \end{pmatrix}, \tag{26}$$

where

$$\overline{f_2}(\tilde{x}, \tilde{y}) = \frac{1}{a_2}\left[a_{11}u^2 + a_{12}uv + a_{22}v^2 \right] + O\left((|x| + |y|)^3 \right),$$

$$\overline{g_2}(\tilde{x}, \tilde{y}) = \left(\frac{a_{11}(\mu - a_1)}{\omega a_2} - \frac{b_{11}}{\omega} \right)u^2 + \left(\frac{a_{12}(\mu - a_1)}{\omega a_2} - \frac{b_{12}}{\omega} \right)uv$$
$$+ \left(\frac{a_{22}(\mu - a_1)}{\omega a_2} - \frac{b_{22}}{\omega} \right)v^2 + O\left((|x| + |y|)^3 \right),$$

and

$$u = a_2\tilde{x}, \quad v = (\mu - a_1)\tilde{x} - \omega\tilde{y},$$
$$u^2 = a_2^2\tilde{x}^2,$$
$$uv = a_2\tilde{x}[(\mu - a_1)\tilde{x} - \omega\tilde{y}],$$
$$v^2 = (\mu - a_1)^2\tilde{x}^2 - 2(\mu - a_1)\omega\tilde{x}\tilde{y} + \omega^2\tilde{y}^2.$$

After that, we characterize the next nonzero real quantities:$\theta = \left[-Re\left(\frac{(1-2\lambda)\overline{\lambda}^2}{1-\lambda}L_{11}L_{12} \right) \right.$
$\left. -\frac{1}{2}|L_{11}|^2 - |L_{21}^2| + Re\left(\overline{\lambda}L_{22} \right) \right]|_{\overline{r^*}=0},$

where

$$L_{11} = \frac{1}{4}\left(\left(\overline{f}_{2\tilde{x}\tilde{x}} + \overline{f}_{2\tilde{y}\tilde{y}} \right) + i\left(\overline{g}_{2\tilde{x}\tilde{x}} + \overline{g}_{2\tilde{y}\tilde{y}} \right) \right),$$

$$L_{12} = \frac{1}{8}\left(\left(\overline{f}_{2\tilde{x}\tilde{x}} - \overline{f}_{2\tilde{y}\tilde{y}} + 2\overline{g}_{2\tilde{x}\tilde{y}} \right) + i\left(\overline{g}_{2\tilde{x}\tilde{x}} - \overline{g}_{2\tilde{y}\tilde{y}} - 2\overline{f}_{2\tilde{x}\tilde{y}} \right) \right),$$

$$L_{21} = \frac{1}{8}\left(\left(\overline{f}_{2\tilde{x}\tilde{x}} - \overline{f}_{2\tilde{y}\tilde{y}} - 2\overline{g}_{2\tilde{x}\tilde{y}} \right) + i\left(\overline{g}_{2\tilde{x}\tilde{x}} - \overline{g}_{2\tilde{y}\tilde{y}} + 2\overline{f}_{2\tilde{x}\tilde{y}} \right) \right),$$

$$L_{22} = \frac{1}{16}\left(\left(\overline{f}_{2\tilde{x}\tilde{x}\tilde{x}} + \overline{f}_{2\tilde{x}\tilde{y}\tilde{y}} + \overline{g}_{2\tilde{x}\tilde{x}\tilde{y}} + \overline{g}_{2\tilde{y}\tilde{y}\tilde{y}} \right) + i\left(\overline{g}_{2\tilde{x}\tilde{x}\tilde{x}} + \overline{g}_{2\tilde{x}\tilde{y}\tilde{y}} - \overline{f}_{2\tilde{x}\tilde{x}\tilde{y}} - \overline{f}_{2\tilde{y}\tilde{y}\tilde{y}} \right) \right).$$

On the basis of this analysis, the following theorem is constructed.

Theorem 5 *Suppose that conditions (24) and $\theta \neq 0$ are satisfied, then model (3) will exhibit N-Sacker bifurcation at the fixed point (x_*, y_*) when r is close to r_2. Further, if $\theta < 0(resp., \theta > 0)$, then an attracting (resp., repelling) invariant closed curve bifurcates from the fixed point for $r > r_2$ (resp., $r < r_2$).*

Existence of Marotto's chaos

Here, we demonstrates how the model (3) shows chaotic behavior in the sense of Marrotto [28]

Definition 1 Assume that the function $F : R^n \rightarrow R^n$ is differentiable in $B_r(Z)$. If $F(Z) = Z$ and all eigenvalues of $DF(X)$ exceed 1 in norm for every $X \in B_r(Z)$, the point $Z \in R^n$ is an expanding fixed point of F in $B_r(Z)$.

Definition 2   For some $r > 0$, let Z be an expanding fixed point of F in $B_r(Z)$. If there exists a point $X_0 \in B_r(Z)$ with $X_0 \neq Z, F^M(X_0) = Z$ and $DF^M(X_0) \neq 0$ for some positive integer M, then Z is said to be a snapback repeller of F.

Firstly, we state the condition that (x_*, y_*) is an expanding fixed point of F. For model (3), we get

$$F(X_n) = \begin{pmatrix} x\exp\left[r(1-x) - \frac{mx^2y}{d+x^2}\right] \\ \alpha x\left[1 - \exp\left(-\frac{mx^2y}{d+x^2}\right)\right] \end{pmatrix}, \quad X_n = \begin{pmatrix} x_n & y_n \end{pmatrix}^T.$$

The eigenvalues associated with (x_*, y_*) are given by

$$\lambda_{1,2} = \frac{R(x_*, y_*) \pm \sqrt{R^2(x_*, y_*) - 4Q(x_*, y_*)}}{2},$$

where

$$R(x_*, y_*) = (1 - rG - L + V),$$

$$Q(x_*, y_*) = N - rGV.$$

We assume that these eigenvalues with (x_*, y_*) are a pair of complex eigenvalues $\lambda, \overline{\lambda}$, and $|\lambda, \overline{\lambda}|$ is greater than unit. This implies to

$$\begin{cases} R^2(x_*, y_*) - 4Q(x_*, y_*) < 0, \\ Q(x_*, y_*) - 1 > 0. \end{cases}$$

Suppose that

$$D_1(x_*, y_*) = R^2(x_*, y_*) - 4Q(x_*, y_*) = (1 - rG - L + V)^2 - 4(N - rGV).$$

Thus $D_1(x_*, y_*) < 0$ if $r \in W_1 = \{(r, d, \alpha, m) \in R_+^4 | r < \frac{4V - (1 - rG - L + V)^2}{4GV}\}$.
Also,

$$D_2(x_*, y_*) = Q(x_*, y_*) - 1 = N - rGV - 1.$$

Thus $D_2(x_*, y_*) > 0$ if $r \in W_2 = \{(r, d, \alpha, m) \in R_+^4 | r < \frac{N-1}{GV}\}$. We summarize the above analysis in the following lemma.

Lemma   3   *If $(x_*, y_*) \in W_1 \cap W_2$,   then $R^2(x_*, y_*) - 4Q(x_*, y_*) < 0$ and $Q(x_*, y_*) - 1 > 0$. Moreover, if the fixed point $z^*(x_*, y_*)$ of model (3) satisfies $z^*(x_*, y_*) \in U_{z^*} = \{(x_*, y_*); (x_*, y_*) \in W_1 \cap W_2\}$. Then, $z^*(x_*, y_*)$ is an expending fixed point in U_{z^*}.*

According to the definition of a snap-back repeller, we need to find one point $z_1(x_1, y_1) \in U_{z^*}$, such that $z_1 \neq z^*, F^M(z_1) = z^*, |DF^M(z_1)| \neq 0$, for some positive integer M, where Map F is defined by (3).
To continue, notice that

$$
\begin{cases}
x_1 \exp\left[r(1 - x_1) - \frac{mx_1^2 y_1}{d + x_1^2}\right] = x_2 \\
\alpha x_1 \left[1 - \exp\left(-\frac{mx_1^2 y_1}{d + x_1^2}\right)\right] = y_2
\end{cases}
\tag{27}
$$

and

$$
\begin{cases}
x_2 \exp\left[r(1 - x_2) - \frac{mx_2^2 y_2}{d + x_2^2}\right] = x_* \\
\alpha x_2 \left[1 - \exp\left(-\frac{mx_2^2 y_2}{d + x_2^2}\right)\right] = y_*
\end{cases}
\tag{28}
$$

Now, a map F^2 has been constructed to map the point $z_1(x_1, y_1)$ to the fixed point $z^*(x_*, y_*)$ after two iterations if there are different solutions from z^* for Eqs. (27) and (17). The various solutions from z^* for Eqs. (17) satisfy the equation below

$$
\begin{cases}
x_2 = \frac{x_*}{\left(1 - \frac{y_*}{\alpha x_2}\right)\exp(r(1 - x_2))}, \\
y_2 = \frac{d + x_2^2}{mx_2^2}\left[\ln\frac{x_2}{x_*} + r(1 - x_2)\right]
\end{cases}
\tag{29}
$$

Substituting x_2 and y_2 into Eq. (27) and solving x_1 and y_1, we have

$$
\begin{cases}
x_1 = \frac{x_2}{\left(1 - \frac{y_2}{\alpha x_1}\right)\exp(r(1 - x_1))}, \\
y_1 = \frac{d + x_1^2}{mx_1^2}\left[\ln\frac{x_1}{x_2} + r(1 - x_1)\right]
\end{cases}
\tag{30}
$$

By simple calculations, we get

$$
\begin{aligned}
\left|DF^2(z_1)\right| = {} & [A + Ax\left(-3mBx^2 + F - 2mBFx^3\right) + mBx^3\left(2Bx + 2BFx^2\right) + r(-D - DFx)] \\
& \times \left[\frac{mDx^2\left(1 - \exp\left(-mBx^3\right)\right)}{d + x^2} - Dx\left(-\frac{2m^2 B^2 x^7}{C^2(d + x^2)} - \frac{-m^2 BN x^5}{C(d + x^2)} + \frac{2m^2 B x^5}{d + x^2}\right)\exp\left(-mBx^3\right)\right] \\
& - \left[Ax\left(-\frac{mx^2}{d + x^2} + mrDx^2 - \frac{2Cm^2 B^2 x^2}{d + x^2} - \frac{m^2 BN x^5}{C(d + x^2)} + \frac{2m^2 x^5 B}{d + x^2}\right)\right] \\
& \times [D(1 - \exp\left(-mBx^3\right)) + DFx\left(1 - \exp\left(-mBx^3\right)\right) - Dx(-3mBx^2 - 2mBFx^3 \\
& + \frac{mBN x^3(F + r)}{C} + mBx^3\left(2D^2 x + 2D^2 Fx^2\right))\exp\left(-mBx^3\right)],
\end{aligned}
$$

where

$$
A = \alpha\exp\left[r(1 - x) + rDx - mBx^3 - \frac{mx^2 y}{d + x^2}\right],
$$

$$
B = \left(\frac{D^2 C}{d + D^2 x^2}\right),
$$

$$
C = \exp\left[1 - \exp\left(\frac{-mx^2 y}{d + x^2}\right)\right],
$$

$$
D = \left(\exp(r(1 - x)) - \frac{mx^2 y}{d + x^2}\right),
$$

$$
F = \left[r - \frac{2mx^3 y}{(d + x^2)^2} - \frac{2mxy}{d + x^2}\right].
$$

Clearly, if lemma 3 is satisfied, the solutions of Eqs. (29) and (30) will furthermore be subject to $z_1(x_1, y_1), z_2(x_2, y_2) \neq z^*(x_*, y_*), z_1(x_1, y_1) \in U_{z^*}$ and $\left| DF^2(z_1) \right| \neq 0$, then z^* is a snap-back repeller in U_{z^*}. As a result, the next theorem is obtained.

Theorem 6 *Let the conditions in lemma 3 hold. Then, the solutions* $z_2(x_2, y_2)$ *and* $z_1(x_1, y_1)$ *of Eqs.* (29) *and* (30) *satisfy in addition* $z_1(x_1, y_1), z_2(x_2, y_2) \neq (x_*, y_*), z_1(x_1, y_1) \in U_{z^*}, z_1(x_1, y_1) \neq (0, 0)$ *and* $\left| DF^2(z_1) \right| \neq 0$, *then* $z^*(x_*, y_*)$
is a snap-back repeller of model (3), *and therefore model* (3) *is chaotic in the sense of Marotto.*

In Sect. Results and discussion related to numerical simulation, we choose specific parametric values to demonstrate the presence of conditions in Theorem 6.

Chaos control

Here, the state delayed feedback control method [29–31] will be used to stabilize the chaotic orbit at an unstable fixed point of the model (3). The controlled form of model (3) can be written as follows:

$$
\begin{cases}
x_{n+1} = x_n \exp\left[r(1 - x_n) - \frac{m x_n^2 y_n}{d + x_n^2} \right] + \delta(x_n - x_{n-1}), \\
y_{n+1} = \alpha x_n \left[1 - \exp\left(-\frac{m x_n^2 y_n}{d + x_n^2} \right) \right]
\end{cases}
\tag{31}
$$

where δ is the feedback gain for the controlled model (31).

After that, we introduce $u_n = x_n - x_{n-1}$ to get the next controlled model, which is equivalent to model (31):

$$
\begin{cases}
x_{n+1} = x_n \exp\left[r(1 - x_n) - \frac{m x_n^2 y_n}{d + x_n^2} \right] + \delta u_n, \\
y_{n+1} = \alpha x_n \left[1 - \exp\left(-\frac{m x_n^2 y_n}{d + x_n^2} \right) \right], \\
u_{n+1} = x_n \left(\exp\left[r(1 - x_n) - \frac{m x_n^2 y_n}{d + x_n^2} \right] - 1 \right) + \delta u_n,
\end{cases}
\tag{32}
$$

The generalized Jacobian matrix of controlled model (32) calculated at the fixed point (x_*, y_*, u_*) is given as:

$$
J(x_*, y_*, u_*) =
\begin{pmatrix}
\left(1 - r x_* - \frac{2 d m x_*^2 y_*}{(d + x_*^2)^2} \right) \exp\left[r(1 - x_*) - \frac{m x_*^2 y_*}{d + x_*^2} \right] & \frac{-m x_*^3}{d + x_*^2} \exp\left[r(1 - x_*) - \frac{m x_*^2 y_*}{d + x_*^2} \right] & \delta \\
\alpha \left[1 - \exp\left(\frac{-m x_*^2 y_*}{d + x_*^2} \right) \right] + \frac{2 m d \alpha x_*^2 y_*}{(d + x_*^2)^2} \exp\left(-\frac{m x_*^2 y_*}{d + x_*^2} \right) & \frac{m \alpha x_*^3}{d + x_*^2} \exp\left(\frac{-m x_*^2 y_*}{d + x_*^2} \right) & 0 \\
\left(-r x_* - \frac{2 d m x_*^2 y_*}{(d + x_*^2)^2} \right) \exp\left[r(1 - x_*) - \frac{m x_*^2 y_*}{d + x_*^2} \right] & \frac{-m x_*^3}{d + x_*^2} \exp\left[r(1 - x_*) - \frac{m x_*^2 y_*}{d + x_*^2} \right] & \delta
\end{pmatrix}
\tag{33}
$$

The characteristic equation of $J(x_*, y_*, u_*)$ is given as

$$
F(\lambda) = \lambda^3 + \hat{A} \lambda^2 + \hat{B} \lambda + \hat{C},
\tag{34}
$$

where

$$\hat{A} = -1 + rG + L - \delta - V, \hat{B} = \delta(1 + V) - rGV - LV + N + \frac{LV}{\alpha}, \hat{C} = -\delta V. \tag{35}$$

Keeping in mind that the model (31) is controllable, we have the next lemma.

Lemma 4   *Suppose that $d + 1 < m\alpha$, then the fixed point (x_*, y_*, u_*) of model (31) is a sink if the following conditions are satisfied*:

$$\begin{aligned}
&\left|\hat{A} + \hat{C}\right| < 1 + \hat{B}, \\
&\left|\hat{A} - 3\hat{C}\right| < 3 - \hat{B}, \\
&\hat{C}^2 + \hat{B} - \hat{A}\hat{C} < 1.
\end{aligned} \tag{36}$$

Results and discussion

Numerical examples and discussion

This section presents bifurcation diagrams, phase portraits, and maximum Lyapunov exponents (MLE) to validate our analytical results and demonstrate the complicated dynamics of the model (3).

Example   1 We choose $d = 4$, $\alpha = 2$, and $m = 10$ with   initial   condition $(x_0, y_0) = (0.683, 0.728)$ and suppose r changes in the interval $[2, 3.5]$. According-ing to Theorem 2, we know that model (3) has only one positive fixed point $(x_*, y_*) = (0.683204, 0.0.727583)$ at $r \approx 2.4$. Furthermore, the characteristic equation of the linearized model (3) estimated at (x_*, y_*) is given by:

$$P(\lambda) = \lambda^2 + 1.33453\lambda + 0.334533. \tag{37}$$

The   roots   of   (37)   are   given   by $\lambda_1 = -1$ and $\lambda_2 = -0.332993$ with $|\lambda_2| \neq 1$ and $(d, \alpha, m, r) \in FB$. From Fig. 1a, b, we see that model (3) undergoes flip bifurcation at $r \approx 2.4$. The bifurcation diagrams of model (3) for x_n, y_n shows that when $r < 2.4$, the fixed point is stable, at $r \approx 2.4$, it becomes unstable and periodic oscillations appear in the range $2.4 \leq r \leq 2.59$, which ultimately leads to chaos. In Fig. 1c, the maximal Lya-punov exponent is plotted to confirm the existence of chaotic behavior. Keeping in view Fig. 1c, we are able to split the interval $[2, 3.5]$ into two sub-intervals, one being a non-chaotic area where all the MLE are negative and it is indicated by $[2, 2.59]$, and the other being a chaotic area and it is indicated by $[2.59, 3.5]$, where some MLE are positive and others are negative. In addition, the chaotic area is larger than the non-chaotic area. Arguing as in [32], the changing MLE signs confirmed that in the chaotic area $[2.59, 3.5]$, there are stable fixed points or stable periodic windows.

Example   2 Fixing $d = 1.4$, $\alpha = 2$, and $m = 10$ with   initial   condition $(x_0, y_0) = (0.514, 0.679)$. Hence, using Theorem 2, the model (3) has a positive fixed point $(x_*, y_*) = (0.514265, 0.678663)$ at $r \approx 2.22$. Also, the characteristic equation of model (3) evaluated at $(0.514265, 0.678663)$ is described by
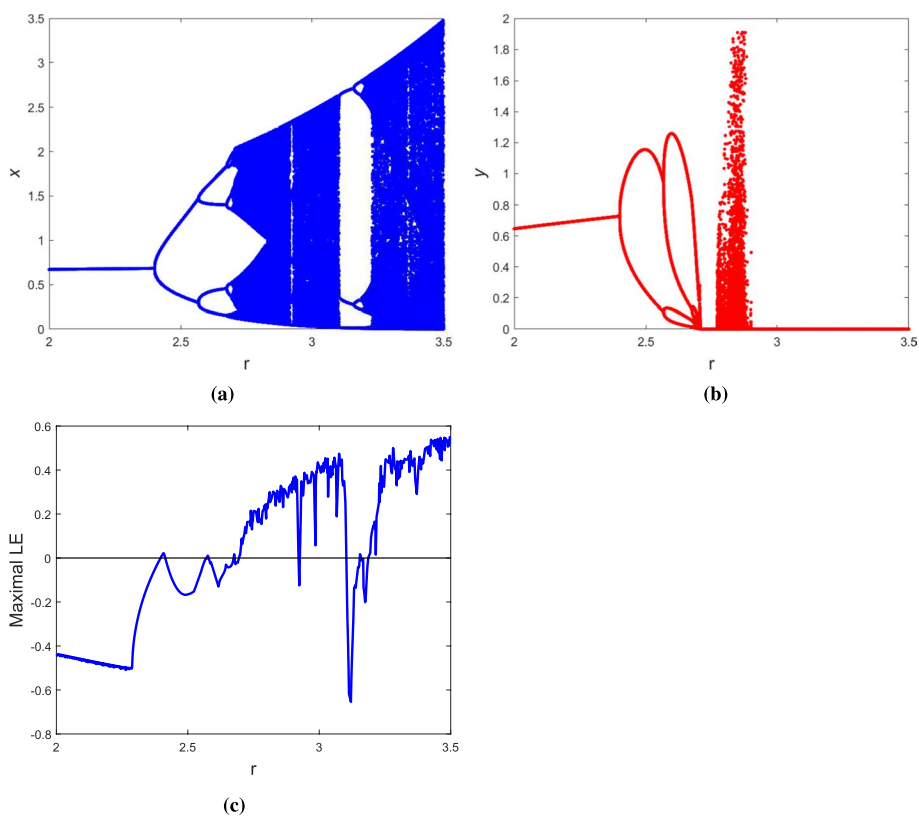
Fig. 1 Flip bifurcation diagrams and MLE for model (3) with $d=4$, $a=2$, $m=10$, $2 \leq r \leq 3.5$ and (x0,y0) = (0.683, 0.728)

$$P(\lambda) = \lambda^2 + 1.39899\lambda + 1.$$

Further, $P(\lambda)$ has a pair of conjugate complex roots $\lambda_{1,2} = -0.699876 \pm 0.713969i$ with $|\lambda_{1,2}| = 1$ and $(r, m, d, \alpha) \in NS$. As a result of Theorem 5, a Neimark–Sacker bifurcation occurs at $r \approx 2.22$. Figure 2a, b shows the bifurcation diagrams for model (3). In addition, the MLE are plotted in Fig. 2c. These MLE confirm the existence of chaotic behavior. Figure 3 shows various phase portraits for model (3). From Fig. 3a, it is clear that the unique positive fixed point $(x_*, y_*) = (0.514265, 0.678663)$ of the model (3) is locally asymptotically stable. Further, at $r \approx 2.22$, the fixed point E_* becomes unstable, and a closed invariant curve containing the unstable fixed point E_* is formed. This indicates the existence of Neimark–Sacker bifurcation at $r \approx 2.22$ (see Fig. 3b). The radii of these closed curves increase as r rises, as shown in Fig. 3c, d. The closed invariant curve vanishes at $r = 2.4733$, and orbits with periods of k form, as shown in Fig. 3e. At $r \approx 2.5822$, an attractive chaotic set forms, as seen in Fig. 3f.

Example 3 Here, we illustrate the existence of Marotto's chaos in model (3). Taking $r = 2.5822$, $d = 1.4$, $m = 10$, and $\alpha = 2$. Also, the fixed point E_* has the form $z^*(2.43, 3.21)$ and the eigenvalues related to this fixed point are $\lambda_{1,2} = -0.79301 \pm 0.516882i$. From Lemma 3, we have $z^* \in U = \{(x_*, y_*); (x_*, y_*) \in W_1 \cap W_2\}$ i.e. z^* is expanding fixed point. Further, there is a fixed point $z_1(x_1, y_1) = (0.614365, 0.746553)$ such that
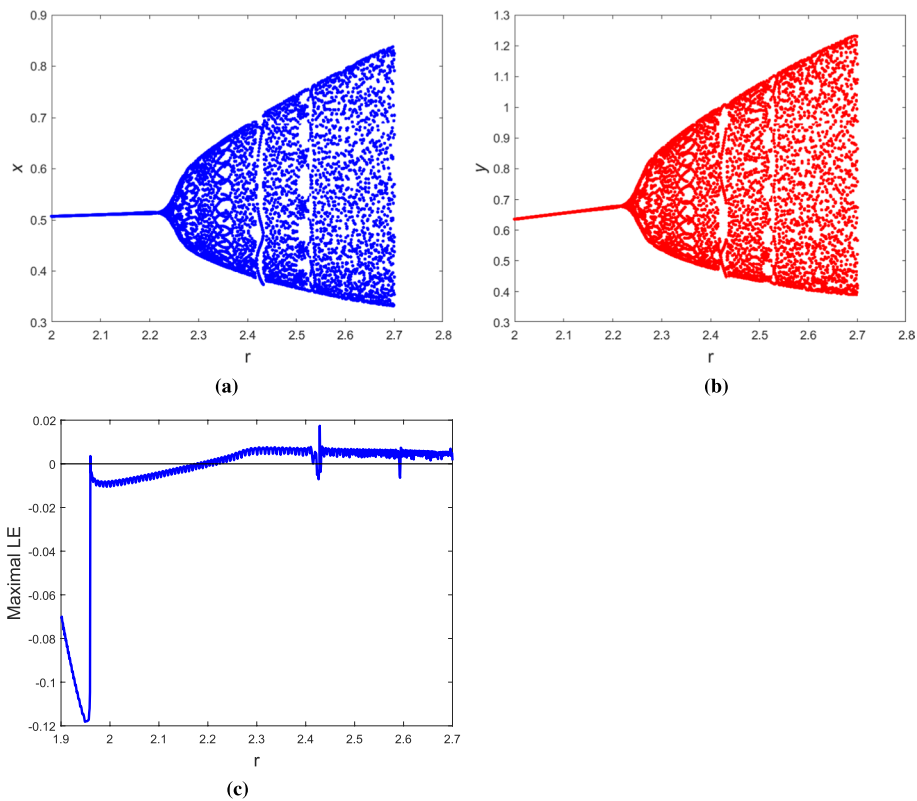
Fig. 2 N-Sacker bifurcation diagrams and MLE for model (3) with $d = 1.4$, $a = 2$, $m = 10$, $2 \leq r \leq 2.7$ and $(x0,y0) = (0.514, 0.679)$

$F^2(z_1) = z^*$ and $\left| DF^2(z_1) \right| \neq 0$. Thus, z^* is snapback repeller. Figure 4 shows the chaotic attractor associated with these parametric values.

Example 4   Finally, we illustrate the effectiveness of the delayed feedback control strategy for the model (3). Taking $m = 10$, $\alpha = 2$, $d = 1.4$, and $r = 2.55$ in the chaotic region. Then, model (3) has a unique positive fixed point $(x_*, y_*) = (0.524796, 0.73716)$, and the characteristic equation for the Jacobian matrix has a pair of conjugate complex roots $\lambda_{1.2} = -0.924898 \pm 0.427348i$ with $|\lambda_{1.2}| = 1.01885 > 1$. Thus, $E_* = (0.524796, 0.73716)$ is a source of model (3). Then, model (32) can be written as:

$$
\begin{cases}
x_{n+1} = x_n \exp\left[2.55(1 - x_n) - \dfrac{10x_n^2 y_n}{1.4 + x_n^2} \right] + \delta u_n, \\[2mm]
y_{n+1} = 2x_n \left[1 - \exp\left(-\dfrac{10x_n^2 y_n}{1.4 + x_n^2} \right) \right], \\[2mm]
u_{n+1} = x_n \left(\exp\left[2.55(1 - x_n) - \dfrac{10x_n^2 y_n}{1.4 + x_n^2} \right] - 1 \right) + \delta u_n,
\end{cases}
\tag{38}
$$

The characteristic equation of the Jacobian matrix of (38) is given by:

$$
\lambda^3 + (1.8498 - \delta)\lambda^2 + (0.518015 + 1.51359\delta)\lambda - 0.513588\delta = 0.
$$
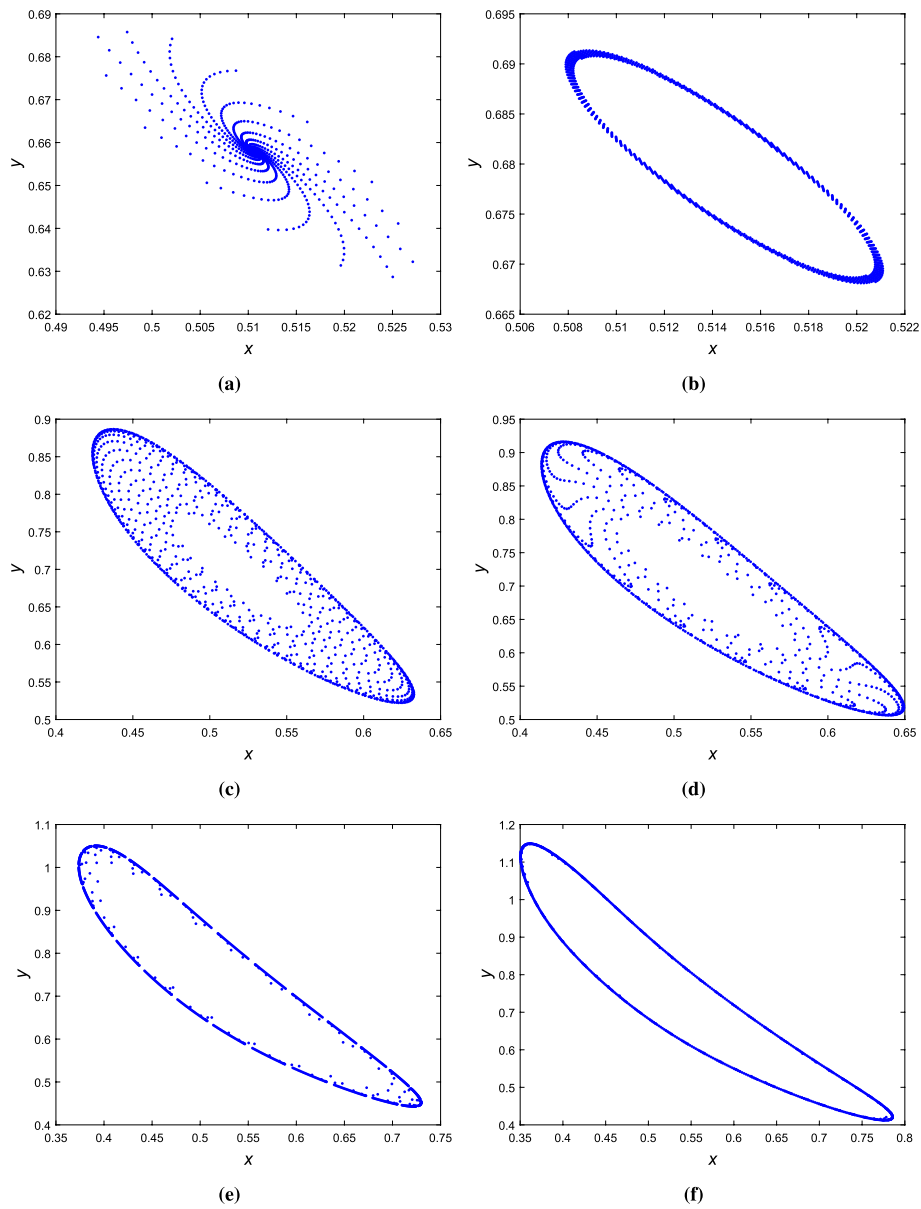
Fig. 3 Phase portraits of model (3) for different values of r with $d = 1.4$, $m = 10$, $a = 2$, $2 \leq r \leq 2.7$ and and initial conditions (x0,y0) = (0.514, 0.679). Phase portrait for **a** $r = 2.111$, **b** $r = 2.22$, **c** $r = 2.31664$, **d** $r = 2.34055$, **e** $r = 2.4732$ and **f** $r = 2.5822$

From Lemma 4, we have E_* is a sink if $0.05 < \delta < 0.1650491$. Thus, model (38) is controllable for $\delta \in]0.05, 0.1650491[$. The controllable region related to these parametric values is shown in Fig. 5.

Conclusion

In this work, we investigated the complicated dynamic behaviors of a host–parasitoid model with Holling type III functional response. Firstly, the existence and stability of the positive fixed point are derived. We then studied the bifurcation behavior of the model
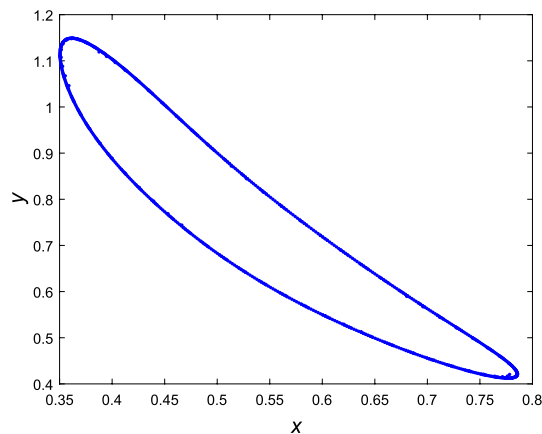
Fig. 4 The Marotto's chaotic attractor for (3) with $d=1.4$, $m=10$, $a=2$, and $r=2.5822$
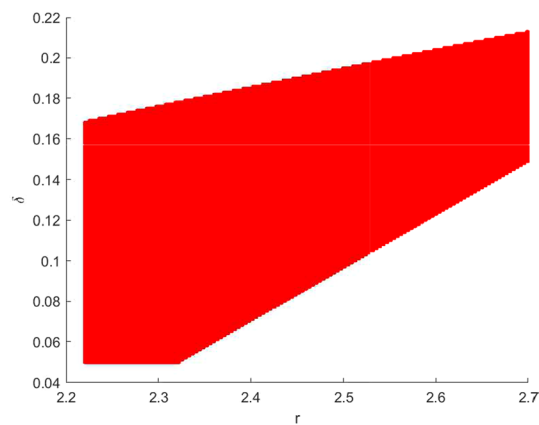
Fig. 5 Controllability region of model (32) with $d=1.4$, $a=2$, $m=10$ and $r \in [2.22, 2.7]$

(3) by applying a perturbation method and the center manifold theorem. Consequently, it is analytically demonstrated that the model presents chaotic behavior in the sense of Marotto. Chaos control of the model (3) is performed by the state-delayed feedback control method. Finally, examples with numerical simulations are carried out to confirm our analytical findings. Our results show that our suggested model has rich features and complicated dynamics. Also, we find that when a simplified Holling type III functional response is included, the area of chaos is reduced when compared to host–parasitoid models with the functional response that was examined by [33]. So, the Holling type III functional response could be seen, at least in part, as a stabilizing effect. Therefore, the Holling type III functional response leads to a direct density dependence when host density is low and thus can lead to the stabilization of host–parasitoid interactions. Thus, natural enemies that display a Holling Type III response are more effective at organizing hosts because they can find hosts at lower densities. This research helps to understand the dynamic behavior of host–parasitoid interactions with an intraspecific competition that may be used to improve classical biological pest control.

Generally, many biological scientists have developed many complex nonlinear mathematical models to describe population dynamics and interactions. However, biologists

are generally frustrated by such mathematical models' analytical intractability. The method used can be regarded as a different approach to the problem.

Declarations

References
1. Allen, L.J.: Introduction to Mathematical Biology. Prentice Hall, New Jersey (2007)
2. Brauer, F., Castillo-Chavez, C.: Mathematical Models in Population Biology and Epidemiology, vol. 2. Springer (2012)
3. Elaydi, S: Dynamics of first-order difference equations, An Introduction to Difference Equations, pp. 1–55, (2005)
4. Guckenheimer, J., Holmes, P.: Nonlinear Oscillations, Dynamical Systems, and Bifurcations of Vector Fields, vol. 42. Springer Science and Business Media (2013)
5. Mohamad, S., Naim, A.: Discrete-time analogues of integrodifferential equations modelling bidirectional neural networks. J. Comput. Appl. Math. **138**(1), 1–20 (2002). https://doi.org/10.1016/S0377-0427(01)00366-1
6. Nicholson, A. J., Bailey, V.A: The balance of animal populations.: part I. in Proceedings of the zoological society of London. vol 105, pp. 551–598. Wiley Online Library (1935). https://doi.org/10.1111/j.1096-3642.1935.tb01680.x.
7. Yousef, A.: Stability and further analytical bifurcation behaviors of Moran–Ricker model with delayed density dependent birth rate regulation. J. Comput. Appl. Math. **355**, 143–161 (2019). https://doi.org/10.1016/j.cam.2019.01.012
8. Yousef, A., Salman, S., Elsadany, A.: Stability and bifurcation analysis of a delayed discrete predator-prey model. Int. J. Bifurc. Chaos. **28**(9), 1850116 (2018). https://doi.org/10.1142/S021812741850116X
9. Thompson, W.: La theorie mathematique de l'action des parasites entomophages et le facteur du hasard. Annu Fac Sci Mars **2**, 69–89 (1924)
10. Yousef, A., Rida, S., Arafat, S.: Stability, analytic bifurcation structure and chaos control in a mutual interference host–parasitoid model. Int. J. Bifurc. Chaos. **30**(15), 2050237 (2020). https://doi.org/10.1142/S0218127420502375
11. Liu, H., Zhang, K., Ye, Y., Wei, Y., Ma, M.: Dynamic complexity and bifurcation analysis of a host–parasitoid model with Allee effect and Holling type III functional response. Adv. Differ. Equ. **2019**(1), 1–20 (2019). https://doi.org/10.1186/s13662-019-2430-8
12. Wu, D., Zhao, H.: Global qualitative analysis of a discrete host–parasitoid model with refuge and strong Allee effects. Math. Methods Appl. Sci. **41**(5), 2039–2062 (2018). https://doi.org/10.1002/mma.4731
13. Din, Q., Hussain, M.: Controlling chaos and Neimark–Sacker bifurcation in a host–parasitoid model. Asian J. Control **21**, 1202–1215 (2019). https://doi.org/10.1002/asjc.1809
14. Din, Q., Gumus, O.A., Khalil, H.: Neimark–Sacker bifurcation and chaotic behaviour of a modified host–parasitoid model. Zeitschrift fur Naturforschung A **72**, 25–37 (2017). https://doi.org/10.1515/zna-2016-0335
15. Liu, X., Chu, Y., Liu, Y.: Bifurcation and chaos in a host–parasitoid model with a lower bound for the host. Adv. Differ. Equ. **2018**, 31 (2018). https://doi.org/10.1186/s13662-018-1476-3
16. Ringel, M., Rees, M., Godfray, H.: The evolution of diapause in a coupled host–parasitoid system. J. Theor. Biol. **194**, 195–204 (1998). https://doi.org/10.1006/jtbi.1998.0754
17. Zhao, M., Zhang, L., Zhu, J.: Dynamics of a host–parasitoid model with prolonged diapause for parasitoid. Commun. Nonlinear Sci. Numer. Simul. **16**, 455–462 (2011). https://doi.org/10.1016/j.cnsns.2010.03.011
18. Liu, H., Li, Z., Gao, M., Dai, H., Liu, Z.: Dynamics of a host–parasitoid model with Allee effect for the host and parasitoid aggregation. Ecol. Complex. **6**, 337–345 (2009)

19. Zhang, L., Zhao, M.: Dynamic complexities in a hyperparasitic system with prolonged diapause for host. Chaos Solit. Fract. **42**, 1136–1142 (2009). https://doi.org/10.1016/j.chaos.2009.03.007
20. Holling, C.: S: Some characteristics of simple types of predation and parasitism. Can. Entomol. **91**, 385–398 (1959). https://doi.org/10.4039/Ent91385-7
21. Hassell, M.: The Spatial and Temporal Dynamics of Host–Parasitoid Interactions. OUP Oxford (2000)
22. van Baalen, M., Krivan, V., van Rijn, P.C.J., Sabelis, M.W.: Alternative food, switching predators, and the persistence of predator prey systems. Am Nat **157**(5), 512–524 (2001). https://doi.org/10.1086/319933
23. Yang, X.: Uniform persistence and periodic solutions for a discrete predator-prey system with delays. J. Math. Anal. Appl. **316**, 161–177 (2006). https://doi.org/10.1016/j.jmaa.2005.04.036
24. Dhar, J., Singh, H., Bhatti, H.S.: Discrete-time dynamics of a system with crowding effect and predator partially dependent on prey. Appl. Math. Comput. **252**, 324–335 (2015). https://doi.org/10.1016/j.amc.2014.12.021
25. Choo, Y.: An elementary proof of the Jury test for real polynomials. Automatica **47**, 249–252 (2011). https://doi.org/10.1016/j.automatica.2010.10.040
26. Kuznetsov, Y.: A: Elements of Applied Bifurcation Theory, vol. 112. Springer Science and Business Media (2013)
27. Wiggins, S.: Introduction to Applied Nonlinear Dynamical Systems and Chaos, vol. 2. Springer Science and Business Media (2003)
28. Marotto, F.R.: On redefining a snap-back repeller. Chaos Solitons Fract. **25**, 25–28 (2005). https://doi.org/10.1016/j.chaos.2004.10.003
29. Ott, E., Grebogi, C., Yorke, J.A.: Controlling chaos. Phys. Rev. Lett. **64**, 1196 (1990). https://doi.org/10.1103/PhysRevLett.64.1196
30. Romeiras, F.J., Grebogi, C., Ott, E., Dayawansa, W.: Controlling chaotic dynamical systems. Phys. D **58**, 165–192 (1992). https://doi.org/10.1016/0167-2789(92)90107-X
31. Robinson, C.: Dynamical Systems: Stability, Symbolic Dynamics, and Chaos. CRC Press (1998)
32. He, Z., Jiang, X.: Bifurcation and chaotic behaviour of a discrete-time variable-territory predator-prey model. IMA J. Appl. Math. **76**, 899–918 (2011). https://doi.org/10.1093/imamat/hxr006
33. Tang, S., Chen, L.: Chaos in functional response host–parasitoid ecosystem models. Chaos Solit. Fract. **13**, 875–884 (2002)

Publisher's Note